PETROLEUM EXPLORATION AND DEVELOPMENT
Volume 52, Issue 1, February 2025
http://www.sciencedirect.com/journal/petroleum-exploration-and-development

Available online at www.sciencedirect.com
ScienceDirect

Cite this article as: PETROL. EXPLOR. DEVELOP., 2025, 52(1): 143–156.

RESEARCH PAPER

Control of structure and fluid on ultra-deep fault-controlled carbonate fracture-vug reservoirs in the Tarim Basin, NW China

ZENG Lianbo[1, 2, *], SONG Yichen[1, 2], HAN Jun[3], HAN Jianfa[4], YAO Yingtao[1, 2], HUANG Cheng[3], ZHANG Yintao[4], TAN Xiaolin[1, 2], LI Hao[1, 2]

1. National Key Laboratory of Petroleum Resources and Engineering, China University of Petroleum (Beijing), Beijing 102249, China;
2. College of Geosciences, China University of Petroleum (Beijing), Beijing 102249, China;
3. Northwest Oilfield Company, Sinopec, Urumqi 830011, China;
4. PetroChina Tarim Oilfield Company, Korla 841000, China

Abstract: This study comprehensively uses various methods such as production dynamic analysis, fluid inclusion thermometry and carbon-oxygen isotopic compositions testing, based on outcrop, core, well-logging, 3D seismic, geochemistry experiment and production test data, to systematically explore the control mechanisms of structure and fluid on the scale, quality, effectiveness and connectivity of ultra-deep fault-controlled carbonate fractured-vuggy reservoirs in the Tarim Basin. The results show that reservoir scale is influenced by strike-slip fault scale, structural position, and mechanical stratigraphy. Larger faults tend to correspond to larger reservoir scales. The reservoir scale of contractional overlaps is larger than that of extensional overlaps, while pure strike-slip segments are small. The reservoir scale is enhanced at fault intersection, bend, and tip segments. Vertically, the heterogeneity of reservoir development is controlled by mechanical stratigraphy, with strata of higher brittleness indices being more conducive to the development of fractured-vuggy reservoirs. Multiple phases of strike-slip fault activity and fluid alterations contribute to fractured-vuggy reservoir effectiveness evolution and heterogeneity. Meteoric water activity during the Late Caledonian to Early Hercynian period was the primary phase of fractured-vuggy reservoir formation. Hydrothermal activity in the Late Hercynian period further intensified the heterogeneity of effective reservoir space distribution. The study also reveals that fractured-vuggy reservoir connectivity is influenced by strike-slip fault structural position and present in-situ stress field. The reservoir connectivity of extensional overlaps is larger than that of pure strike-slip segments, while contractional overlaps show worse reservoir connectivity. Additionally, fractured-vuggy reservoirs controlled by strike-slip faults that are nearly parallel to the present in-situ stress direction exhibit excellent connectivity. Overall, high-quality reservoirs are distributed at the fault intersection of extensional overlaps, the central zones of contractional overlaps, pinnate fault zones at intersection, bend, and tip segments of pure strike-slip segments. Vertically, they are concentrated in mechanical stratigraphy with high brittleness indices.

Key words: structure and fluid; fractured-vuggy reservoir; strike-slip fault; mechanical stratigraphy; carbonate rock; ultra-deep layer; Tarim Basin

Introduction

The ultra-deep (buried depth over 6 000 m) Middle–Lower Ordovician fault-controlled carbonate reservoirs in the Tarim Basin have favorable hydrocarbon accumulation conditions and abundant hydrocarbon sources, making them a key target for increasing reserves and production in the platform area of the Tarim Basin [1–2]. Multi-scale fractures, vugs and pore systems controlled by multi-phase strike-slip faulting and fluid activities serve as the primary reservoir space and govern the scale and quality of ultra-deep carbonate fractured-vuggy reservoirs [3–5]. However, the complex interplay of multi-phase tectonic activity and fluid modifications has led to significant variations in the scale, quality, and effectiveness of

Received date: 03 Apr. 2024; **Revised date:** 07 Jan. 2025.
*** Corresponding author.** E-mail: lbzeng@cup.edu.cn
Foundation item: Supported by the National Natural Science Foundation of China (U21B2062).
https://doi.org/10.1016/S1876-3804(25)60010-3
Copyright © 2025, Research Institute of Petroleum Exploration and Development Co., Ltd., CNPC (RIPED). Publishing Services provided by Elsevier B.V. on behalf of KeAi Communications Co., Ltd. This is an open access article under the CC BY-NC-ND license (http://creativecommons.org/licenses/by-nc-nd/4.0/).

reservoirs across different structural positions, resulting in pronounced heterogeneity. A comprehensive investigation into the genesis and distribution of these reservoirs, driven by tectonic and fluid activities, is crucial, with particular emphasis on the differential accumulation of ultra-deep fractured-vuggy carbonate reservoirs. The findings contribute to a better understanding of the development patterns and provide valuable guidance for hydrocarbon exploration and development of ultra-deep carbonate reservoirs in the Tarim Basin. [6–8].

In recent years, growing attention has been given to understanding the mechanisms and spatial distribution of fractured-vuggy carbonate reservoirs from the perspectives of tectonic deformation and fluid activity [9–12]. In the Tarim Basin, fractures generated by ultra-deep fault activity, along with dissolution pores within fracture zones, have formed distinctive fault-controlled karst reservoirs [13]. These reservoirs exhibit significant genetic differences from conventional fractured-porous reservoirs. Their formation cannot be fully explained by a single reservoir-forming mechanism, such as meteoric water infiltration, organic acid dissolution, or sulfate reduction-related processes. This highlights the complexity of the mechanisms of ultra-deep fractured-vuggy carbonate reservoirs [14]. The evolution of these reservoirs is governed by multiple factors, including stratigraphic sequences, lithofacies, structural deformation, fluid activity, paleogeomorphology, and geological time. Among these factors, the sustained activity of strike-slip faults and fluid processes during reservoir formation and deep burial are regarded as key controls in understanding the development patterns of ultra-deep, large-scale fractured-vuggy carbonate reservoirs [11, 15–17]. Characterizing the coupled mechanisms of these controlling factors and predicting reservoir effectiveness and connectivity remain critical scientific challenges in fault-controlled hydrocarbon exploration and development within the ultra-deep formations of the Tarim Basin.

The concept of structural diagenesis was first introduced by Laubach et al. to describe the interaction between deformation processes or structures and the chemical alterations in sediments [18]. A typical manifestation of this concept is mineral cementation and fracture filling occurring during deformation. This framework has been applied to investigate the evolution of natural fracture porosity. Zeng et al. proposed that structural diagenesis encompasses the interaction between deformation and diagenetic processes throughout the transition of sedimentary rocks from an unconsolidated state to lithification and beyond [19]. Using this approach, they examined the differential evolution mechanisms of deep to ultra-deep tight sandstone reservoirs in foreland basins and assessed reservoir quality. Currently, numerous studies have focused on the influence of structural diagenesis in controlling tight sandstone reservoirs [20–23]. However, research on ultra-deep fractured-vuggy carbonate reservoirs remains in its infancy. Existing studies primarily focus on the evolution of fault zones and the impacts of compaction and dissolution on reservoir properties. The dynamic interactions between structural deformation and fluid activity governing the development of ultra-deep fractured-vuggy carbonate reservoirs remain unclear [24–25]. Fault activity induced by regional tectonics, along with associated fractures that control dissolution and diagenetic cementation driven by fluid activity, also falls within the scope of structural diagenesis (referred to as structural and fluid processes in this study). Investigating the controls exerted by structure and associated fluid processes on the formation and evolution of fractured-vuggy carbonate reservoirs could provide a theoretical geological basis for predicting the distribution of fault-controlled fractured-vuggy reservoirs.

This study integrates data from outcrops, cores, well logs, mud logs, 3D seismic surveys, geochemical experiments, and production tests, employing various methods such as production performance analysis, fluid inclusion thermometry, and carbon-oxygen isotope testing to systematically investigate how structural deformation and fluid processes control the scale, quality, effectiveness, and connectivity of ultra-deep fault-controlled fractured-vuggy carbonate reservoirs. The findings aim to enhance the understanding of the development mechanisms of ultra-deep fault-controlled fractured-vuggy carbonate reservoirs in the Tarim Basin and provide valuable insights for guiding hydrocarbon exploration and development.

1. Geologic setting

The Tarim Basin is the largest inland basin in China, bounded by the South Tianshan Mountains, Kunlun Mountains, and Altun Mountains. It is a large composite basin formed by the superposition of prototype basins from different geological periods and with diverse genetic origins. Structurally, the basin is divided into 12 units, commonly referred to as the "five uplifts, six depressions, and one slope". From north to south, these structural units include the Kuqa Depression, Tabei Uplift, Awati Depression, Shuntuoguole Low Uplift, Manjiaer Depression, Bachu Uplift, Tazhong Uplift, Tadong Uplift, Maigaiti Slope, Tangubasi Depression, Southwest Depression, and Southeast Depression [26] (Fig. 1a). Ultra-deep fractured-vuggy carbonate reservoirs are primarily distributed along the northern slope of the Tazhong Uplift, Shuntuoguole Low Uplift, Tabei Uplift, and Maigaiti Slope. This study focuses on the Tabei Uplift, Shuntuoguole Low Uplift, and the northern slope of the Tazhong Uplift (Fig. 1b).

The ultra-deep fractured-vuggy carbonate reservoirs in the Tarim Basin are primarily developed within the Middle to Lower Ordovician Yingshan and Yijianfang formations (Fig. 1c). The Yijianfang Formation represents an open-platform depositional system. The lower member of the Yijianfang Formation (Y1) is characterized by intershoal sea and intra-platform deposits, primarily composed

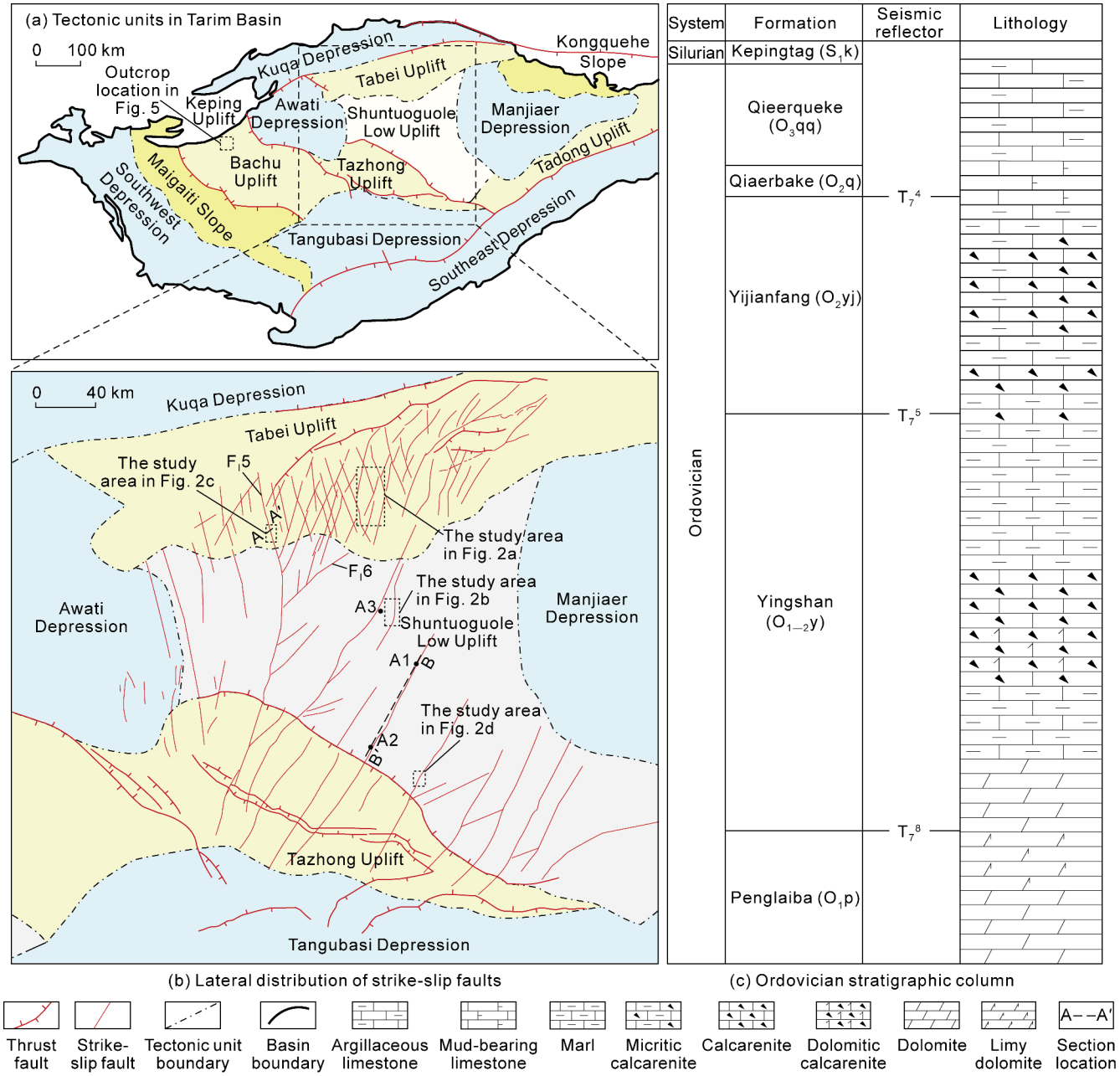

Fig. 1. Structural framework and stratigraphic distribution of northern-central Tarim Basin (modified from Reference [26]).

of calcarenite, micritic calcarenite and marl. The upper submember (Y2) is characterized by tidal flat, mud mound, and inter-mound sea deposits, with local development of intra-platform. The predominant lithologies include marl and micritic calcarenite. The Yingshan Formation records the transition from a restricted to an open marine depositional environment. During the deposition of Y1, the water conditions were relatively confined, leading to the formation of semi-restricted to restricted platform facies. The lithology of Y1 is characterized by calcarenite, dolomitic calcarenite, marl and dolomite. With the onset of Y2, as sea level rose, the depositional environment became more open, developing an open-platform facies dominated by pure micrite [27].

2. Strike-slip faults

Ultra-deep strike-slip faults are widely distributed across the platform area of the Tarim Basin, especially the northern Tarim Basin (Tabei in brief) and the central Tarim Basin (Tazhong in brief) have been investigated frequently (Fig. 1b). In map view, these strike-slip faults predominantly exhibit NNE–SSW and NNW–SSE orientations [28]. Conjugate strike-slip faults are well-developed in the Tabei Uplift (Fig. 2a), whereas single-orientation faults dominate the northern slope of the Tazhong Uplift and the Shuntuoguole Low Uplift [29]. In map view, these faults exhibit notable segmentation, including pure strike-slip segments, fault tips, bends, and overlapping segments [30–31]. The pure strike-slip segments are characterized by linear extension along the major fault, accompanied by short branch faults in the surrounding areas, forming diverse structural patterns such as linear, en-echelon and pinnate structures [28, 32]. Linear structures are distributed in parallel in areas with low stress release

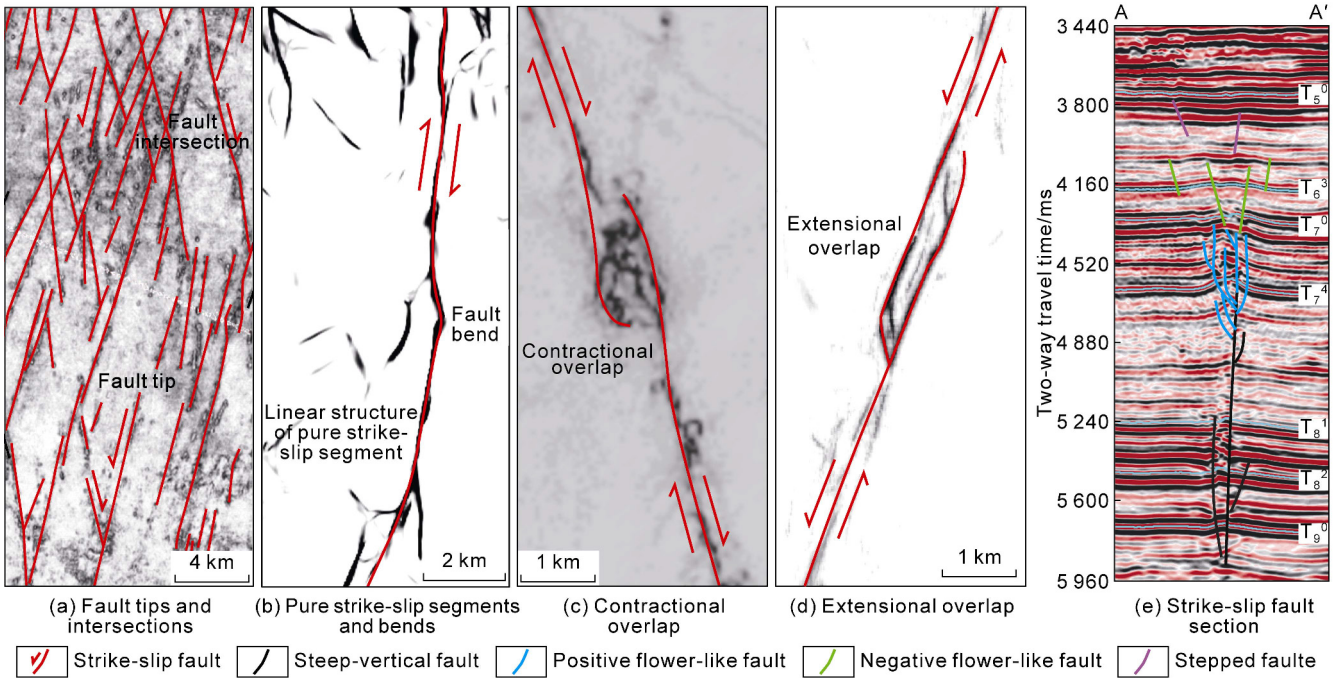

Fig. 2. Typical deformation characteristics of ultra-deep strike-slip faults in the Tarim Basin (see the plane and profile locations in Fig. 1b). T_9^0—Cambrian bottom; T_8^2—Middle Cambrian Awatage Formation gypsum-salt rock bottom; T_8^1—Middle Cambrian Awatage Formation gypsum-salt rock top; T_7^4—Middle Ordovician top; T_7^0—Ordovician top; T_6^3—Lower Silurian Kepingtag Formation top; T_5^0—Permian top.

(Fig. 2b), while en-echelon structures exhibit step-like arrangements [33–34]. Pinnate structures symmetrically extend outward from the major fault [33, 35]. The fault tips are located at the points where the faults on either side are about to disappear (Fig. 2a) and display structural patterns such as pinnate faults, horsetail faults, synthetic branch faults, and antithetic faults [30]. Pinnate faults intersect the major fault at high angles and extend short distances, exhibiting large displacements and feather-like openings. In contrast, horsetail faults intersect the major fault at low angles and extend over longer distances [29, 31]. Bends are distinct curvatures along continuous fault planes, where the stress state is either compressional or extensional [36–37] (Fig. 2b). Overlapping segments result from the superposition of two en-echelon pure strike-slip segments and can be classified as strong overlaps or weak overlaps. Strong overlaps exhibit a fan-shaped geometry laterally and converge into flower structures vertically, whereas weak overlaps are nearly parallel with limited overlap [38–40]. Based on their arrangement and slip direction, these overlaps can be further classified as contractional or extensional overlaps [41]. When the arrangement opposes the slip direction, the stress state is compressional, resulting in the formation of narrow back-thrust bulges (Fig. 2c). Conversely, when the arrangement aligns with the slip direction, the stress state is extensional, leading to the development of pull-apart depressions (Fig. 2d) [42].

Vertically, the strike-slip faults exhibit layered deformation characteristics (Fig. 2e). In the Cambrian–Middle Ordovician (T_9^0–T_7^4) carbonate rocks, the faults are steep to nearly vertical, with occasional small branches. In the Upper Ordovician (T_7^4–T_7^0) mudstones, plastic deformation dominates without faults. Upward, a series of positive flower structures is observed [7, 28, 34]. In the Silurian–Permian (T_6^3–T_5^0) clastic rocks, multiple extensional normal faults have two distinct structural patterns: negative flower structures and step-like structures. The superposition of these structures with positive flower structures formed by multi-phase faulting resulted in multi-layered flower structures [7, 43] (Fig. 2e). Multi-phase and multi-segment fault activity led to diverse planar and vertical characteristics of the strike-slip faults, forming a complex fracture network [26, 30], which significantly controlled fluid migration and dissolution, and consequently reservoir development and hydrocarbon accumulation [43–44].

3. Control of strike-slip faults and mechanical stratigraphy on fractured-vuggy reservoirs

3.1. Control of strike-slip faults

A strike-slip fault is a binary structure consisting of a fault core and a damage zone. The damage zone refers to the fracture zone controlled by the fault [45–47], and its scale determines the extent of fractured-vuggy reservoirs. The fracture zone is quantitatively characterized by a fracture development index, which is calculated using seismic attributes (e.g., automatic fault detection, coherence, etc.) [26]. The fracture development index is high near the fault and stably becomes low as apart from the

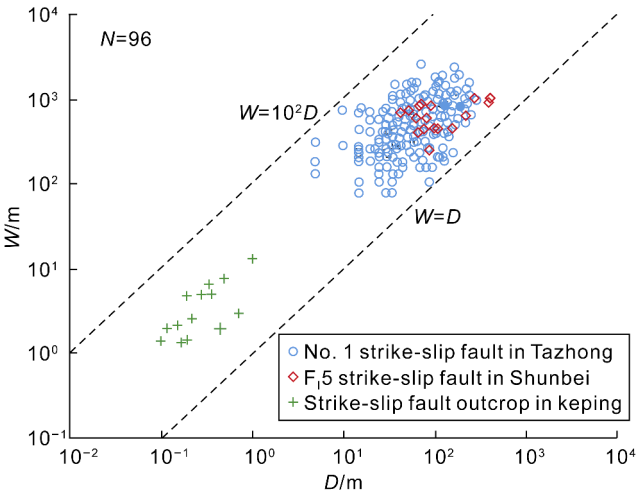

Fig. 3. Width of damaged zone vs. fault displacement of strike-slip faults in the Tarim Basin (modified from references [48–49]; *W*—width of damaged zone; *D*—fault displacement; *N*—number of samples).

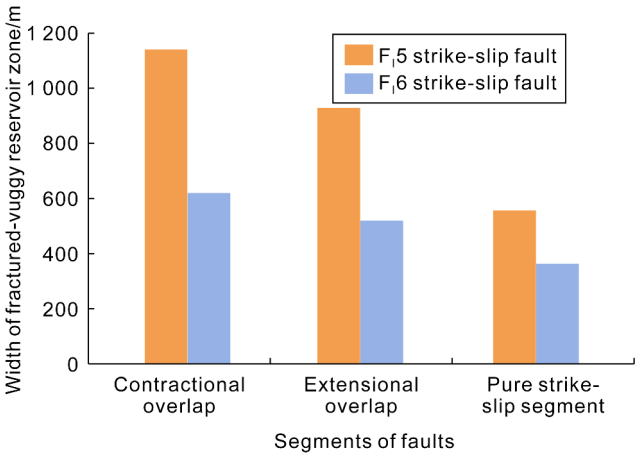

Fig. 4. Statistical width of fractured-vuggy reservoir zones controlled by different segments of ultra-deep strike-slip faults in northern and central Tarim Basin (see fault locations in Fig. 1b).

fault, indicating that the fault no longer controls fracture development. Outcrop and seismic data indicate that the width of the damage zone is closely related to fault scale and intensity. Larger and more active faults generate wider damage zones, which in turn lead to the formation of larger fractured-vuggy reservoirs [26, 48–49] (Fig. 3). For example, in the central–northern Tarim Basin, the large F$_1$5 fault (Fig. 1b) controls fractured-vuggy reservoirs 500 m to 1 100 m wide, while the small F$_1$6 fault (Fig. 1b) controls reservoirs only 350 m to 600 m wide (Fig. 4).

Laterally, there are significant differences in the width of fracture development zones and the degree of fracture development at different structural positions along strike-slip faults [30]. In overlapping segments, fractures are densely developed [50]. Strong overlapping segments, characterized by stress release and large slip displacements, generate wider fracture zones with diverse orientations, enhancing fracture connectivity and making these areas favorable for the development of fractured-vuggy reservoirs. In contrast, weak overlapping segments exhibit smaller slip displacements and less fracture development [34]. Contractional overlaps display more complex fracture structures, wider fracture development zones, and larger reservoir development scales compared to extensional overlaps [30, 51]. In pure strike-slip segments, both the width and the degree of fracture development are smaller than those in overlapping segments. Fault intersections and bends exhibit stress concentration, leading to a higher degree of fracture development. Fault tips are also zones of fracture development, where fractures associated with pinnate faults have shorter extensions than those of horsetail faults but possess better connectivity. These features contribute to the formation of highly permeable fracture networks and favor the development of fractured-vuggy reservoirs [33].

3.2. Control of mechanical stratigraphy

Vertically, the scale of fractured-vuggy reservoirs controlled by strike-slip faults varies significantly across different strata, primarily governed by mechanical stratigraphy (Fig. 5). Mechanical stratigraphy refers to a stratigraphic unit with similar mechanical strength, brittleness, and faulting mechanical properties, comprising a mechanical unit and two mechanical interfaces [52–53]. Mechanical stratigraphy typically controls the formation and distribution of fractures, which generally develop within a mechanical unit but terminate or are impeded at mechanical interfaces [54–55]. Based on well logging and core data from 11 wells in the Middle–Lower Ordovician carbonate reservoirs in the study area, the lithological and fracture characteristics of the Yingshan and Yijianfang formations were systematically analyzed.

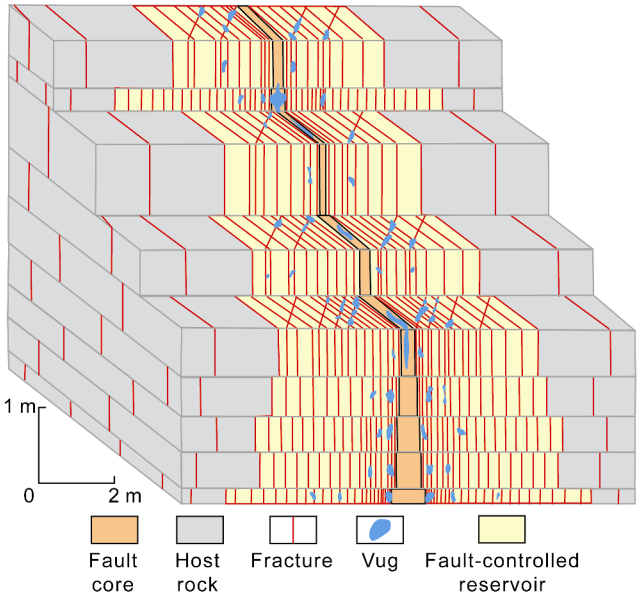

Fig. 5. 3D structural model of strike-slip faults in an outcrop area (see the outcrop location in Fig. 1a).

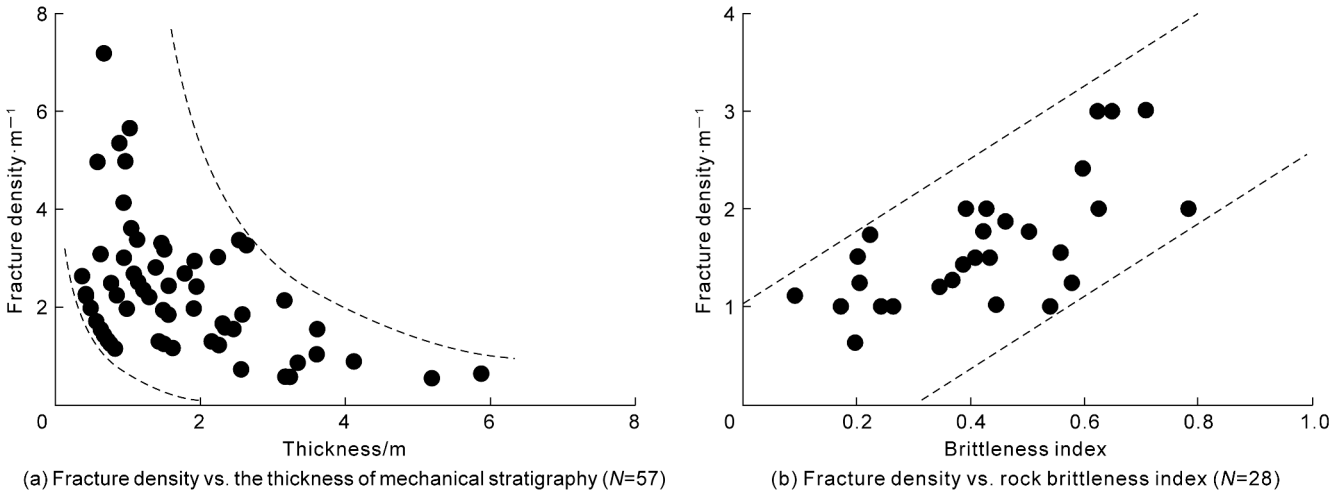

(a) Fracture density vs. the thickness of mechanical stratigraphy (*N*=57)

(b) Fracture density vs. rock brittleness index (*N*=28)

Fig. 6. Fracture density vs. mechanical stratigraphy thickness and brittleness index in ultra-deep carbonate reservoirs in the Tarim Basin.

The vertical mechanical stratigraphy was finely divided, and the relationship between fracture density and the thickness of the mechanical stratigraphy was investigated. Statistical results indicate that the thinner the mechanical stratigraphy, the higher the fracture density (Fig. 6a).

The brittleness index is a critical parameter for evaluating the brittleness of mechanical stratigraphy [55]. Variations in fracture development lead to differences in fluid activity and dissolution, which in turn influence the width and quality of fault-controlled fractured-vuggy reservoirs. Using acoustic curves (AC) and density logging curves, the brittleness index can be calculated through an integrated mechanical parameter method [55], guiding the division of mechanical stratigraphy. Based on the brittleness index and fracture density statistics from 11 wells in the study area, the results indicate that higher brittleness indices correspond to greater fracture densities (Fig. 6b). The mechanical interfaces, where significant changes in mechanical properties occur, can be identified at the inflection points of abrupt changes in the brittleness index curve. Using this method, two mechanical stratigraphies were identified in the Yijianfang Formation, and three were identified in the Yingshan Formation (Fig. 7). Among these, the 5th mechanical stratigraphy exhibits the highest brittleness index and the most significant fracture development. In contrast, the 1st and 4th mechanical stratigraphies show moderate brittleness indices and fracture development, while the 2nd and 3rd mechanical stratigraphies have low brittleness indices and minimal fracture development. Overall, in the Yingshan Formation, as burial depth increases, the dolomite and clastic content gradually increase, resulting in a higher brittleness index and more pronounced fracture development. This trend is particularly evident in the lower member of the Yingshan Formation, where the fifth mechanical stratigraphy exhibits the highest brittleness index and more extensive fracture development, making it the most favorable zone for fractured-vuggy reservoirs.

4. Control of fluid on the effectiveness of fractured-vuggy reservoirs

The development degree, effectiveness and connectivity of fractures and vugs determine the quality of fractured-vuggy reservoirs [56–57]. These characteristics are primarily controlled by multiphase tectonic activities (including strike-slip faults and tectonic stress fields) and fluid-related processes (such as dissolution and cementation). Based on in-situ U-Pb isotopic dating and fluid inclusion thermometry of fracture and vug fillings, and combined with burial history analysis, the fault-controlled fractured-vuggy reservoirs in the Ordovician of the Tarim Basin were mainly formed during the Middle Caledonian, Late Caledonian to Early Hercynian, and Late Hercynian periods [58–60]. The burial depth during the main development phases of fractured-vuggy reservoirs typically did not exceed 4 500 m [61]. After formation, the reservoirs underwent fluid modification which influenced their evolution, effectiveness and connectivity, ultimately resulting in their heterogeneity.

Based on the fluid inclusion thermometry and carbon-oxygen isotope composition analyses of the fracture and vug fillings in the Shunbei area, and considering the oil and gas charging history in the Middle–Lower Ordovician, four periods of fluid activity were identified: (1) Middle Caledonian; (2) Late Caledonian to Early Hercynian; (3) Late Hercynian; and (4) Himalayan (Fig. 8a). Carbon-oxygen isotope measurements reveal that the primary diagenetic fluids represented by the Middle Caledonian inclusions are meteoric water and formation water. In contrast, the Late Caledonian to Early Hercynian inclusions predominantly represents meteoric water, the Late Hercynian inclusions represent hydrothermal fluids, and the Himalayan inclusions are associated

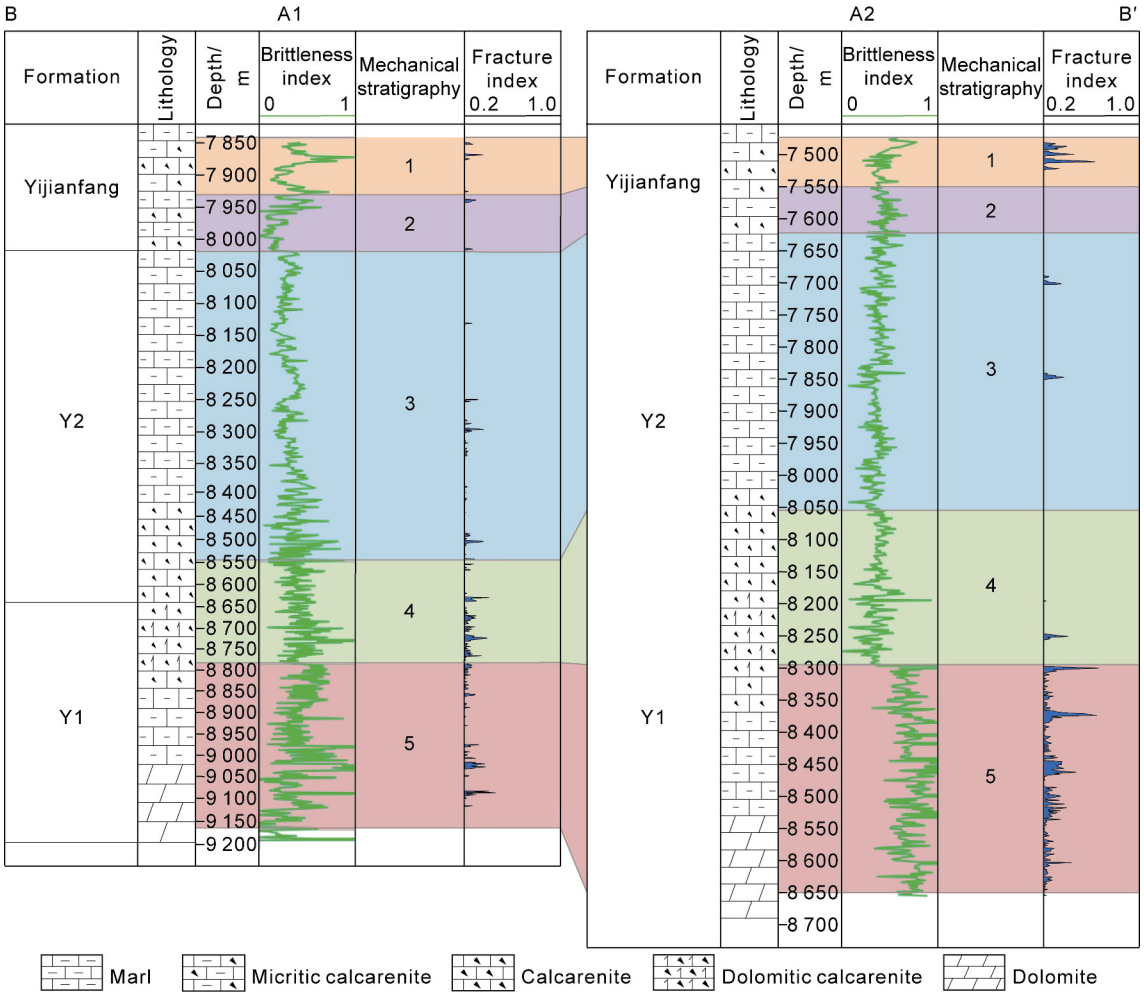

Fig. 7. Vertical distribution of fractures controlled by mechanical stratigraphy in Yingshan Formation–Yijianfang Formation in the Tarim Basin (see well and section locations in Fig. 1b).

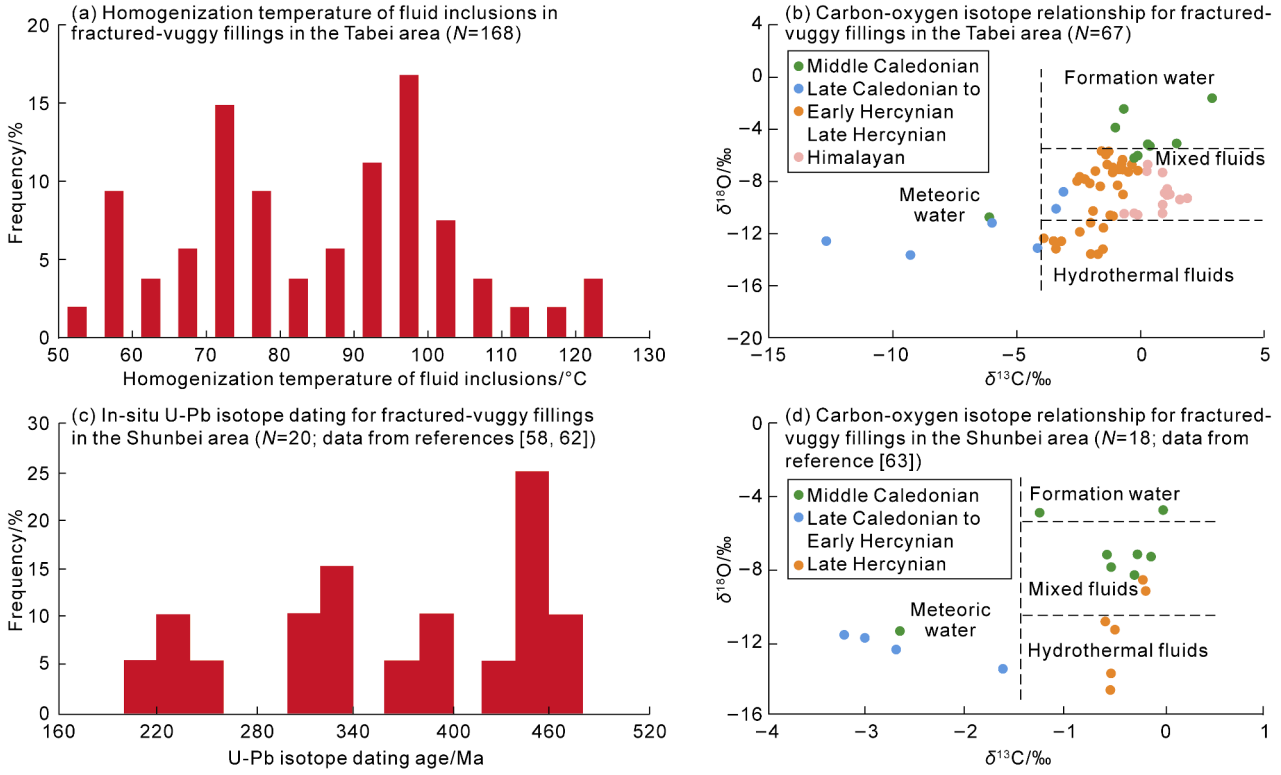

Fig. 8. Fluid inclusion thermometry, carbon-oxygen isotope composition analysis and in-situ U-Pb isotope dating of calcite veins in fault-controlled fractures and vugs in the Tarim Basin (*N*—number of samples).

with mixed fluids of uncertain origin (Fig. 8b). In the Shunbei area, in-situ U-Pb isotopic dating of fracture and vug fillings indicates four periods of fluid activity: (1) Middle Caledonian; (2) Late Caledonian to Early Hercynian; (3) Late Hercynian; and (4) Indosinian [58, 62] (Fig. 8c). The Middle Caledonian fluids are primarily meteoric water and formation water. The Late Caledonian to Early Hercynian fluid is dominated by meteoric water. The Late Hercynian fluid is hydrothermal fluid. The Indosinian fluid lacks a clear source [63] (Fig. 8d). Generally, diagenetic fluid activities happened in four periods: Middle Caledonian, Late Caledonian to Early Hercynian, Late Hercynian and Indosinian–Himalayan. The Middle Caledonian fluids are characterized by meteoric water and formation water. The Late Caledonian to Early Hercynian fluid is primarily meteoric water. The Late Hercynian fluid is dominated by deep hydrothermal fluid. The fluid activity during the Indosinian–Himalayan period was relatively weak, but one to two episodes of hydrocarbon charging occurred, and hydrocarbon-generating organic acid was introduced [64–65].

During the Middle Caledonian period, the Tarim Basin experienced tectonic uplift and sea-level decline, allowing meteoric water to infiltrate carbonate rocks that had not undergone compaction, pressure dissolution, or cementation. As a result, syn-sedimentary to early diagenetic processes formed intragranular dissolution pores, moldic pores, and intergranular dissolution pores in the reservoirs [61, 66–67] (Fig. 9).

From the Late Caledonian to the Early Hercynian, the northern Tarim Basin experienced significant uplift followed by long-term erosion. Extensive epigenetic karstification induced by meteoric water occurred in the eroded areas. Toward the central Tarim Basin, the terrain transitioned into buried hills. Pre-existing strike-slip faults played a crucial role in vertical connectivity, facilitating the downward infiltration of meteoric water along fault zones and through aquitards, leading to the dissolution and modification of carbonate rock [68]. In addition, previous studies have found that the first phase of hydrocarbon charging occurred during the Late Caledonian period. Organic acids generated from the thermal degradation of organic matter migrated upward through fault zones and flowed laterally near early vugs and unconformities, inducing further dissolution and modification [64–65] (Fig. 9). Consequently, large cavernous reservoirs developed in the northern region, while fractured-vuggy reservoirs formed in the central part. The distribution and types of these reservoirs were significantly controlled by geomorphology and fault activity [61].

During the Late Hercynian period, widespread magmatic and volcanic activity occurred across the basin, and a large volume of hydrothermal fluid migrated upward along fault zones. Upon entering the Middle–Lower Ordovician strata, the hydrothermal fluid released acidic gases, such as CO and HS, which dissolved in water, inducing the formation of fractures and vugs [50]. As formation temperature and pressure decreased and oversaturation occurred, coarse calcite crystals precipitated, filling the fractures and vugs [69]. Additionally, deep brine became enriched with silica as it upwelled through the Cambrian and ultimately deposited quartz, dolomite, and calcite in the Middle–Lower Ordovician reservoirs. Deep hydrothermal fluid activity caused the redistribution of effective fractures and vugs, increasing reservoir heterogeneity [70]. This process had a pronounced impact on the fractured-vuggy reservoirs in the northern slope of the Tazhong Uplift and the Shuntuoguole Low Uplift. In contrast, the Tabei Uplift, which is relatively elevated and suffered less volcanic activity, was less affected. Meanwhile, meteoric water continued to infiltrate the Middle–Lower Ordovician and mixed with organic acids generated during the second phase of hydrocarbon charging, leading to further reservoir dissolution [71] (Fig. 9). During the Indosinian–Himalayan period, one to two phases of hydrocarbon charging occurred. Although organic acids contributed to the development of fractured-vuggy reservoirs, their impact was limited due to their small volume and poor flow ability [64–65] (Fig. 9).

In general, from the Late Caledonian to the Early Hercynian, widespread meteoric water dissolution marked the primary formation phase of fractured-vuggy reservoirs, resulting in cavernous reservoirs in the Tabei Uplift and fractured-vuggy reservoirs in the northern slope of the Tazhong Uplift and the Shuntuoguole Low Uplift. The Late Hercynian period served as a critical modification stage for fractured-vuggy reservoirs, during which dissolution and precipitation associated with deep hydrothermal fluids enhanced reservoir heterogeneity. The multi-phase and multi-type fluid activities in the Tarim Basin, involving both dissolution and subsequent cementation, not only controlled the effectiveness of fractured-vuggy carbonate reservoirs but also contributed to multi-scale heterogeneity in reservoir space (Fig. 10).

5. Connectivity and development model of fractured-vuggy reservoirs

5.1. Connectivity and influencing factors

The effectiveness and connectivity of reservoirs in different segments of the strike-slip faults exhibit significant variation due to the influence of multi-phase differential tectonic deformation and fluid modification. Based on 3D seismic interpretation, core fracture statistics and production dynamic data analysis, the extensional overlaps of the strike-slip faults are characterized by a high degree of fracture development and relatively large fracture apertures (2.0–2.5 mm), resulting in the highest effectiveness and connectivity of fractured-vuggy reservoirs. In

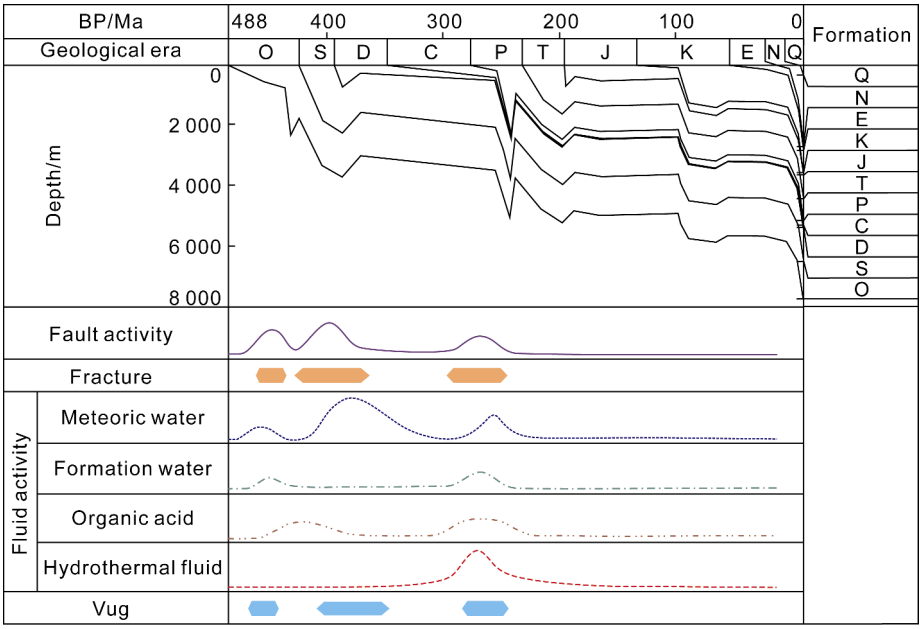

Fig. 9. Effects of fault and fluid activities on the development of fractures and vugs in the Middle–Lower Ordovician in the Tarim Basin. O—Ordovician; S—Silurian; D—Devonian; C—Carboniferous; P—Permian; T—Triassic; J—Jurassic; K—Cretaceous; E—Paleogene; N—Neogene; Q—Quaternary.

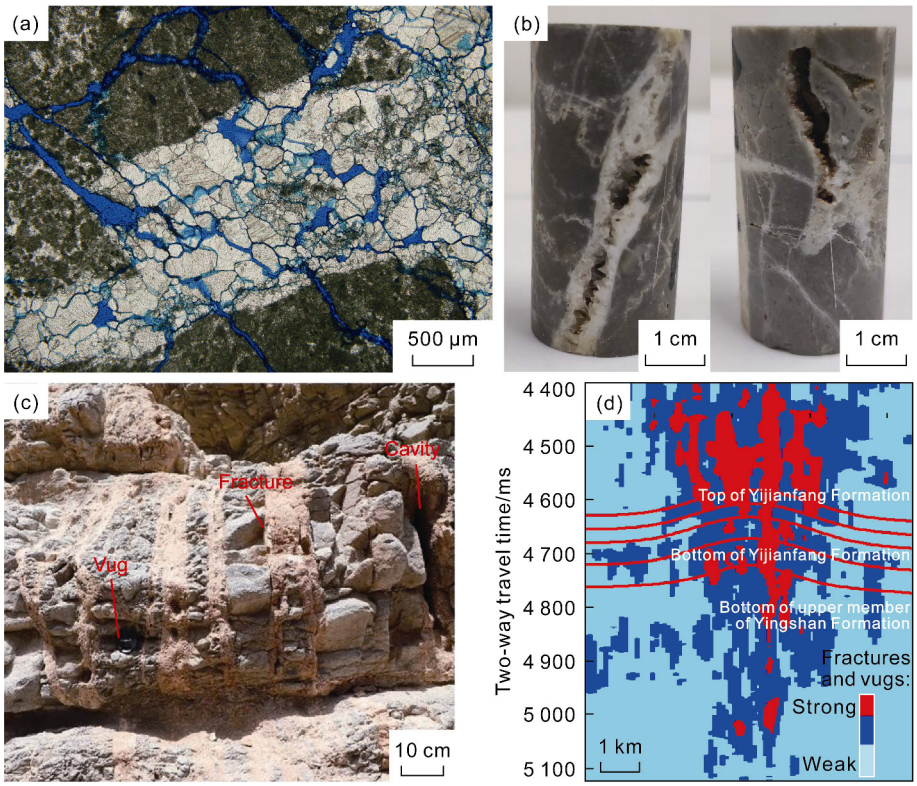

Fig. 10. Multi-scale heterogeneity of the fractured-vuggy reservoirs modified by strike-slip faults and fluid activities in the Tarim Basin. (a) Micron- to millimeter-scale microfractures with intragranular and intercrystalline dissolution pores, Yingshan Formation, 7 982.50 m, Well A3, cast thin section; (b) centimeter- to decimeter-scale fractures and dissolution vugs, Yingshan Formation, 8 076.32 m, Well A3, core sample; (c) meter- to tens of meters-scale faulted cavities, fractures and vugs, Yangjikan section in the Keping outcrop area; (d) hundred meter- to thousand meter-scale faulted cavities and vugs modeled by fractured-vuggy attributes, Shunbei Oilfield.

contrast, although fractures are highly developed in the contractional overlaps, their apertures are much smaller (0.5–1.0 mm), so the reservoirs are isolated to some extent and less effective and connective. The pure strike-slip segments show less fracture development but moderate fracture apertures (1.0–1.5 mm), so the effectiveness and connectivity are moderate, too. Production dynamic data further supported these findings. For instance, in the F$_{\text{I}}$6 strike-slip fault zone in the Shuntuoguole area, the average oil production per unit pressure drop is 6 694 t/MPa

from five production wells in the extensional overlaps, 3 140 t/MPa from six production wells in the pure strike-slip segments, and only 887 t/MPa from one production well in the contractional overlaps (Fig. 11). Moreover, production data confirmed the existence of three types of connected well groups within the F$_1$6 fault zone: the type of "extensional overlap", the type of "pure strike-slip segment", and the type of "extensional overlap and pure strike-slip segment". However, no connected well groups were identified in the "contractional overlap" type. This suggests that the fractured-vuggy reservoirs in the extensional overlaps exhibit better connectivity than the pure strike-slip segments. In contrast, those in the contractional overlaps have relatively poor connectivity [72].

The orientation of strike-slip faults and the direction of present in-situ stress also influence the effectiveness and connectivity of fractured-vuggy reservoirs. When the fault orientation aligns with or intersects at a small angle with the present maximum horizontal principal stress, the normal stress acting on the fractures is relatively low, resulting in larger fracture apertures and better reservoir effectiveness and connectivity. In contrast, when the fault orientation is nearly perpendicular to or intersects at a large angle with the present maximum horizontal principal stress, the normal stress on the fractures increases, leading to smaller fracture apertures and reduced reservoir effectiveness and connectivity. According to the analyses of drilling-induced fractures, the present maximum horizontal principal stress in the central Tarim Basin is oriented in the NE–SW direction. Production dynamic data indicate that the NE–SW trending F$_1$6 fault, which is closely aligned with this stress direction, has confirmed three connected well groups. The average pressure propagation rate between wells is 229 m/h, and the average oil production per unit pressure drop from 12 production wells is 4 433 t/MPa. In contrast, in the NW–SE trending northern section of the F$_1$5 fault, which intersects the present maximum horizontal principal stress at a large angle, the reservoir effectiveness and connectivity are poor despite the wider fracture zone. Only one connected well group was identified, where the average pressure propagation rate is just 9.8 m/h, and the average oil production per unit pressure drop from six production wells is only 895 t/MPa [72] (Fig. 11). This demonstrates that fractured-vuggy reservoirs controlled by NE–SW trending faults which are closely aligned with the present maximum horizontal principal stress exhibit superior effectiveness and connectivity. Such alignment facilitates the interconnection of reservoirs, enabling high and sustainable oil and gas production [51].

5.2. Development model of fractured-vuggy reservoirs

Strike-slip faults predominantly control the formation and distribution of ultra-deep fractured-vuggy reservoirs

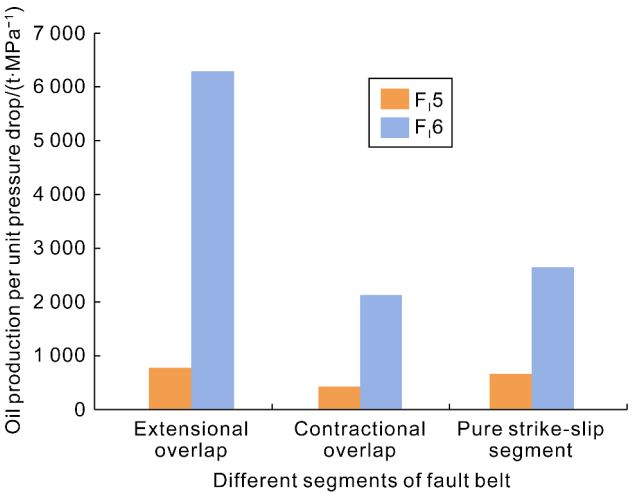

Fig. 11. Oil production per unit pressure drop from production wells at different segments of strike-slip fault (data from reference [72]).

in the Tarim Basin. The activity of strike-slip faults primarily governs the formation and development of the surrounding fracture system. These faults and their associated fracture systems, in turn, control the pattern of fluid migration, thereby influencing the development of vugs in carbonate reservoirs. During the formation and evolution of strike-slip faults, uneven stress distribution leads to significant variations in the development of fracture networks and associated vugs across different fault segments.

Laterally, fractured-vuggy reservoirs are preferentially developed in overlapped segments, fault intersections, bends, and fault tips, where fractures are densely developed, facilitating fluid activity and dissolution that contribute to the formation of high-quality fractured-vuggy reservoirs. These fault segments are characterized by the extensive development of fractured-vuggy reservoirs with superior reservoir quality. Notably, the terminal intersections on both sides of the extensional overlap are more active, resulting in the development of larger-scale and higher-quality fractured-vuggy reservoirs compared to the central part of the extensional overlap. In contrast, within the contractional overlap, the central zone has more extensively developed fractured-vuggy reservoirs. Furthermore, both the extensional overlap and the pinnate fault zone at fault tips are subjected to extensional stress, which facilitates the formation of fracture networks with larger apertures and better permeability. Consequently, the effectiveness and connectivity of fractured-vuggy reservoirs in these areas are significantly enhanced.

Vertically, within mechanical stratigraphy with high brittleness indices, the fractures controlled by strike-slip faults are generally more developed, with larger apertures, providing favorable conditions for the formation and development of fractured-vuggy reservoirs. In contrast,

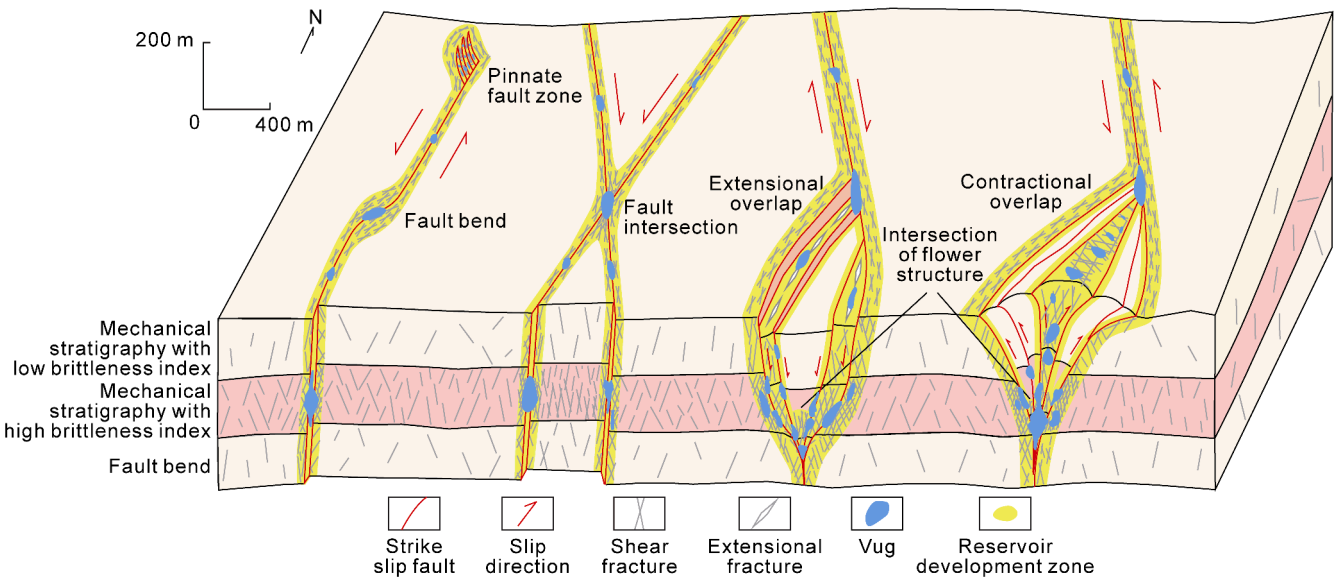

Fig. 12. Development models of fractured-vuggy reservoirs controlled by ultra-deep strike-slip faults in the Tarim Basin.

the scale of fractured-vuggy reservoirs around pure strike-slip segments is relatively limited. The flower-structure areas within overlapping segments, especially at the intersections of major faults and branch faults, are highly favorable for fracture development and fluid-induced dissolution. These areas are, therefore, more likely to host high-quality fractured-vuggy reservoirs (Fig. 12).

6. Conclusions

The primary reservoir space of ultra-deep fault-controlled fractured-vuggy carbonate reservoirs in the Tarim Basin consists of multi-scale fractures and associated vugs controlled by strike-slip faults. Fault scale, structural position, and mechanical stratigraphy jointly control the reservoir scale. Laterally, a larger fault scale and displacement correlate with a larger reservoir scale. Reservoirs in contractional overlaps are more extensive than those in extensional overlaps, but those in pure strike-slip segments are less developed. Fault intersections, fault bends, and tips of single faults facilitate fracture development and are therefore more likely to host larger fractured-vuggy reservoirs. Vertically, mechanical stratigraphy with higher brittleness indices is more favorable for the development of fractured-vuggy reservoirs.

The Late Caledonian to Early Hercynian period marks the primary formation phase for ultra-deep Ordovician fault-controlled fractured-vuggy reservoirs in the Tarim Basin. During this period, meteoric water activity led to the formation of cavernous reservoirs in the Tabei Uplift and fault-controlled fractured-vuggy reservoirs in the northern slope of the Tazhong Uplift and the Shuntuoguole Low Uplift. During the Late Hercynian period, deep hydrothermal fluid activity continued to modify the distribution of effective space in fractured-vuggy reservoirs, enhancing reservoir heterogeneity and impacting reservoir effectiveness and connectivity. The effectiveness and connectivity of fractured-vuggy reservoirs in extensional overlaps are better than those in pure strike-slip segments, while contractional overlaps exhibit relatively poorer effectiveness and connectivity. Strike-slip faults that are nearly parallel to or intersect the present maximum horizontal principal stress at a small angle control fractured-vuggy reservoirs with better connectivity, whereas those that intersect at a large angle result in poorer connectivity.

Laterally, the favorable development zones of ultra-deep fractured-vuggy carbonate reservoirs in the Tarim Basin are primarily located at the terminal intersections on both sides of the extensional overlaps, the central zones of the contractional overlaps, the fault intersections and fault bends of pure strike-slip segments, and the pinnate fault zones at fault tips. Vertically, these reservoirs are predominantly found within mechanical stratigraphy with high brittleness indices, and the lower member of the Yingshan Formation also facilitates the development of fractured-vuggy reservoirs except of Yijianfang Formation.

References

[1] SUN Longde, ZOU Caineng, ZHU Rukai, et al. Formation, distribution and potential of deep hydrocarbon resources in China. Petroleum Exploration and Development, 2013, 40(6): 641–649.

[2] MA Yongsheng, CAI Xunyu, YUN Lu, et al. Practice and theoretical and technical progress in exploration and development of Shunbei ultra-deep carbonate oil and gas field, Tarim Basin, NW China. Petroleum Exploration and Development, 2022, 49(1): 1–17.

[3] LI Bin, ZHONG Li, LYU Haitao, et al. Dynamic simulation of differential accumulation history of deep marine oil and gas in superimposed basin: A case study of Lower Paleo-

zoic petroleum system of Tahe Oilfield, Tarim Basin, NW China. Petroleum Exploration and Development, 2024, 51(5): 1053–1066.

[4] MA Yongsheng, HE Zhiliang, ZHAO Peirong, et al. A new progress in formation mechanism of deep and ultra-deep carbonate reservoir. Acta Petrolei Sinica, 2019, 40(12): 1415–1425.

[5] MA Yongsheng, CAI Xunyu, LI Maowen, et al. Research advances on the mechanisms of reservoir formation and hydrocarbon accumulation and the oil and gas development methods of deep and ultra-deep marine carbonates. Petroleum Exploration and Development, 2024, 51(4): 692–707.

[6] TIAN F, DI Q Y, JIN Q, et al. Multiscale geological-geophysical characterization of the epigenic origin and deeply buried paleokarst system in Tahe Oilfield, Tarim Basin. Marine and Petroleum Geology, 2019, 102: 16–32.

[7] WANG Z Y, GAO Z Q, FAN T L, et al. Structural characterization and hydrocarbon prediction for the SB5M strike-slip fault zone in the Shuntuo Low Uplift, Tarim Basin. Marine and Petroleum Geology, 2020, 117: 104418.

[8] MA Qingyou, ZENG Lianbo, XU Xuhui, et al. Internal architecture of strike-slip fault zone and its control over reservoirs in the Xiaoerbulake section, Tarim Basin. Oil & Gas Geology, 2022, 43(1): 69–78.

[9] BARBIER M, HAMON Y, CALLOT J P, et al. Sedimentary and diagenetic controls on the multiscale fracturing pattern of a carbonate reservoir: The Madison Formation (Sheep Mountain, Wyoming, USA). Marine and Petroleum Geology, 2012, 29(1): 50–67.

[10] GUO Xusheng, HU Dongfeng, HUANG Renchun, et al. Developing mechanism for high quality reef reservoir (Changxing Formation) buried in ultra-depth in the big Yuanba Gas Field. Acta Petrologica Sinica, 2017, 33(4): 1107–1114.

[11] HE Zhiliang, ZHANG Juntao, DING Qian, et al. Factors controlling the formation of high-quality deep to ultra-deep carbonate reservoirs. Oil & Gas Geology, 2017, 38(4): 633–644.

[12] WANG Xiaoyao, ZENG Lianbo, WEI Hehua, et al. Research progress of the fractured-vuggy reservoir zones in carbonate reservoir. Advances in Earth Science, 2018, 33(8): 818–832.

[13] LU Xinbian, HU Wenge, WANG Yan, et al. Characteristics and development practice of fault-karst carbonate reservoirs in Tahe area, Tarim Basin. Oil & Gas Geology, 2015, 36(3): 347–355.

[14] DONG S F, CHEN D Z, ZHOU X Q, et al. Tectonically driven dolomitization of Cambrian to Lower Ordovician carbonates of the Quruqtagh area, north-eastern flank of Tarim Basin, north-west China. Sedimentology, 2017, 64(4): 1079–1106.

[15] ZENG L B, TANG X M, WANG T C, et al. The influence of fracture cements in tight Paleogene saline lacustrine carbonate reservoirs, western Qaidam Basin, northwest China. AAPG Bulletin, 2012, 96(11): 2003–2017.

[16] ZHU D Y, MENG Q Q, JIN Z J, et al. Formation mechanism of deep Cambrian dolomite reservoirs in the Tarim Basin, Northwestern China. Marine and Petroleum Geology, 2015, 59: 232–244.

[17] JIA L Q, CAI C F, WANG Z L, et al. Calcite vein system and its importance in tracing paleowater flow and hydrocarbon migration in the Ordovician carbonates of the Tazhong area, Tarim Basin, China. AAPG Bulletin, 2020, 104(11): 2401–2428.

[18] LAUBACH S E, EICHHUBL P, HILGERS C, et al. Structural diagenesis. Journal of Structural Geology, 2010, 32(12): 1866–1872.

[19] ZENG Lianbo, ZHU Rukai, GAO Zhiyong, et al. Structural diagenesis and its petroleum geological significance. Petroleum Science Bulletin, 2016, 1(2): 191–197.

[20] ZHANG Ronghu, ZENG Qinglu, WANG Ke, et al. New progress in the theory and technology of tectonic diagenesis on reservoir and the geological significance of ultra-deep oil and gas exploration. Acta Petrolei Sinica, 2020, 41(10): 1278–1292.

[21] ZENG Lianbo, LIU Guoping, ZHU Rukai, et al. A quantitative evaluation method of structural diagenetic strength of deep tight sandstone reservoirs in Kuqa foreland basin. Acta Petrolei Sinica, 2020, 41(12): 1601–1609.

[22] LAI J, LI D, AI Y, et al. Structural diagenesis in ultra-deep tight sandstones in the Kuqa Depression, Tarim Basin, China. Solid Earth, 2022, 13(6): 975–1002.

[23] WEI G Q, WANG K, ZHANG R H, et al. Structural diagenesis and high-quality reservoir prediction of tight sandstones: A case study of the Jurassic Ahe Formation of the Dibei gas reservoir, Kuqa Depression, Tarim Basin, NW China. Journal of Asian Earth Sciences, 2022, 239: 105399.

[24] WU G H, XIE E, ZHANG Y F, et al. Structural diagenesis in carbonate rocks as identified in fault damage zones in the northern Tarim Basin, NW China. Minerals, 2019, 9(6): 360.

[25] YU J X, SHI K B, WANG Q Q, et al. Structural diagenesis of deep carbonate rocks controlled by intra-cratonic strike-slip faulting: An example in the Shunbei area of the Tarim Basin, NW China. Basin Research, 2022, 34(5): 1601–1631.

[26] YAO Y T, ZENG L B, MAO Z, et al. Differential deformation of a strike-slip fault in the Paleozoic carbonate reservoirs of the Tarim Basin, China. Journal of Structural Geology, 2023, 173: 104908.

[27] JIAO Cunli, HE Bizhu, WANG Tianyu, et al. Types and quantitative characterization of reservoir spaces of the ultra-deep limestone reservoirs in the Yijianfang Formation during the Middle Ordovician, Shuntuoguole area, Tarim Basin. Acta Petrologica Sinica, 2018, 34(6): 1835–1846.

[28] HAN X Y, DENG S, TANG L J, et al. Geometry, kinematics and displacement characteristics of strike-slip faults in the

northern slope of Tazhong uplift in Tarim Basin: A study based on 3D seismic data. Marine and Petroleum Geology, 2017, 88: 410–427.

[29] LAN X D, LYU X X, ZHU Y M, et al. The geometry and origin of strike-slip faults cutting the Tazhong low rise megaanticline (central uplift, Tarim Basin, China) and their control on hydrocarbon distribution in carbonate reservoirs. Journal of Natural Gas Science and Engineering, 2015, 22: 633–645.

[30] KIM Y S, PEACOCK D C P, SANDERSON D J. Fault damage zones. Journal of Structural Geology, 2004, 26(3): 503–517.

[31] LI H, LIN C Y, REN L H, et al. Quantitative prediction of multi-period tectonic fractures based on integrated geological-geophysical and geomechanics data in deep carbonate reservoirs of Halahatang Oilfield in northern Tarim Basin. Marine and Petroleum Geology, 2021, 134: 105377.

[32] WU J, FAN T L, GAO Z Q, et al. A conceptual model to investigate the impact of diagenesis and residual bitumen on the characteristics of Ordovician carbonate cap rock from Tarim Basin, China. Journal of Petroleum Science and Engineering, 2018, 168: 226–245.

[33] NENG Yuan, YANG Haijun, DENG Xingliang. Structural patterns of fault broken zones in carbonate rocks and their influences on petroleum accumulation in Tazhong Paleo-uplift, Tarim Basin, NW China[J]. Petroleum Exploration and Development, 2018, 45(1): 40–50.

[34] DENG S, LI H L, ZHANG Z P, et al. Structural characterization of intracratonic strike-slip faults in the central Tarim Basin. AAPG Bulletin, 2019, 103(1): 109–137.

[35] QIU H B, DENG S, ZHANG J B, et al. The evolution of a strike-slip fault network in the Guchengxu High, Tarim Basin (NW China). Marine and Petroleum Geology, 2022, 140: 105655.

[36] BURCHFIEL B C, STEWART J H. "Pull-apart" origin of the central segment of death valley, California. GSA Bulletin, 1966, 77(4): 439–442.

[37] CUNNINGHAM W D, MANN P. Tectonics of strike-slip restraining and releasing bends. Geological Society, London, Special Publications, 2007, 290(1): 1–12.

[38] MILLER R B. A mid-crustal contractional stepover zone in a major strike-slip system, North Cascades, Washington. Journal of Structural Geology, 1994, 16(1): 47–60.

[39] WESTAWAY R. Deformation around stepovers in strike-slip fault zones. Journal of Structural Geology, 1995, 17(6): 831–846.

[40] WANG Qinghua, YANG Haijun, WANG Rujun, et al. Discovery and exploration technology of fault-controlled large oil and gas fields of ultra-deep formation in strike-slip fault zone in Tarim Basin. China Petroleum Exploration, 2021, 26(4): 58–71.

[41] QI L X. Structural characteristics and storage control function of the Shun I fault zone in the Shunbei region, Tarim Basin. Journal of Petroleum Science and Engineering, 2021, 203: 108653.

[42] BIAN Q, DENG S, LIN H X, et al. Strike-slip salt tectonics in the Shuntuoguole Low Uplift, Tarim Basin, and the significance to petroleum exploration. Marine and Petroleum Geology, 2022, 139: 105600.

[43] JIA Chengzao, MA Debo, YUAN Jingyi, et al. Structural characteristics, formation & evolution and genetic mechanisms of strike-slip faults in the Tarim Basin. Natural Gas Industry, 2021, 41(8): 81–91.

[44] YANG Haijun, DENG Xingliang, ZHANG Yintao, et al. Great discovery and its significance of exploration for Ordovician ultra-deep fault-controlled carbonate reservoirs of Well Manshen 1 in Tarim Basin. China Petroleum Exploration, 2020, 25(3): 13–23.

[45] CHESTER F M, LOGAN J M. Composite planar fabric of gouge from the Punchbowl Fault, California. Journal of Structural Geology, 1987, 9(5/6): IN5–IN6.

[46] CHESTER F M, EVANS J P, BIEGEL R L. Internal structure and weakening mechanisms of the San Andreas Fault. Journal of Geophysical Research: Solid Earth, 1993, 98(B1): 771–786.

[47] CHOI J H, EDWARDS P, KO K, et al. Definition and classification of fault damage zones: A review and a new methodological approach. Earth-Science Reviews, 2016, 152: 70–87.

[48] MA D B, WU G H, SCARSELLI N, et al. Seismic damage zone and width–throw scaling along the strike-slip faults in the Ordovician carbonates in the Tarim Basin. Petroleum Science, 2019, 16(4): 752–762.

[49] ZHAO Z, LIU J T, DING W L, et al. Analysis of seismic damage zones: A case study of the Ordovician formation in the Shunbei 5 fault zone, Tarim Basin, China. Journal of Marine Science and Engineering, 2021, 9(6): 630.

[50] WANG X T, WANG J, CAO Y C, et al. Characteristics, formation mechanism and evolution model of Ordovician carbonate fault-controlled reservoirs in the Shunnan area of the Shuntuogole lower uplift, Tarim Basin, China. Marine and Petroleum Geology, 2022, 145: 105878.

[51] YUN Lu. Controlling effect of NE strike-slip fault system on reservoir development and hydrocarbon accumulation in the eastern Shunbei area and its geological significance, Tarim Basin. China Petroleum Exploration, 2021, 26(3): 41–52.

[52] GROSS M R, FISCHER M P, ENGELDER T, et al. Factors controlling joint spacing in interbedded sedimentary rocks: Integrating numerical models with field observations from the Monterey Formation, USA. Geological Society, London, Special Publications, 1995, 92(1): 215–233.

[53] ZENG Lianbo, ZHAO Jiyong, ZHU Shengju, et al. Study on the influence of rock heterogeneity on fracture development. Progress in Natural Science, 2008, 18(2): 216–220.

[54] CHEN J J, HE D F, TIAN F L, et al. Control of mechanical stratigraphy on the stratified style of strike-slip faults in the central Tarim Craton, NW China. Tectonophysics, 2022, 830: 229307.

[55] CAO Dongsheng, ZENG Lianbo, HUANG Cheng, et al. Control of multi-scale mechanical stratigraphy on development of faults and fractures. Earth Science, 2023, 48(7): 2535–2556.

[56] DONG Shaoqun, ZENG Lianbo, DU Xiangyi, et al. An intelligent prediction method of fractures in tight carbonate reservoirs. Petroleum Exploration and Development, 2022, 49(6): 1179–1189.

[57] YAO Yingtao, ZENG Lianbo, ZHANG Hang, et al. Fracture development laws of Feixianguan Formation carbonate reservoirs in Huanglongchang-Qilibei area, northeast Sichuan. Earth Science, 2023, 48(7): 2643–2651.

[58] WANG Bin, YANG Yi, CAO Zicheng, et al. U-Pb dating of calcite veins developed in the Middle-Lower Ordovician reservoirs in Tahe Oilfield and its petroleum geologic significance in Tahe Oilfield. Earth Science, 2021, 46(9): 3203–3216.

[59] YANG P, WU G H, NURIEL P, et al. In situ LA-ICPMS U-Pb dating and geochemical characterization of fault-zone calcite in the central Tarim Basin, northwest China: Implications for fluid circulation and fault reactivation. Chemical Geology, 2021, 568: 120125.

[60] LI Huili, GAO Jian, CAO Zicheng, et al. Spatial-temporal distribution of fluid activities and its significance for hydrocarbon accumulation in the strike-slip fault zones, Shuntuoguole low-uplift, Tarim Basin. Earth Science Frontiers, 2023, 30(6): 316–328.

[61] ZENG L B, SONG Y C, LIU G P, et al. Natural fractures in ultra-deep reservoirs of China: A review. Journal of Structural Geology, 2023, 175: 104954.

[62] WU Guanghui, MA Bingshan, HAN Jianfa, et al. Origin and growth mechanisms of strike-slip faults in the central Tarim cratonic basin, NW China. Petroleum Exploration and Development, 2021, 48(3): 510–520.

[63] WANG Yuwei, CHEN Honghan, CAO Zicheng, et al. Controlling effects of fluid activity on reservoir formation in Shunbei area. Fault-Block Oil and Gas Field, 2023, 30(1): 44–51.

[64] LIU Yongli, LUO Mingxia, XIA Yongtao, et al. Geochemical evidence for hydrocarbon accumulation in deep Ordovician in TS3 well block, Tahe oil field. Petroleum Geology and Experiment, 2017, 39(3): 377–382.

[65] LIU Jianzhang, CAI Zhongxian, TENG Changyu, et al. Coupling relationship between formation of calcite veins and hydrocarbon charging in Middle-Lower Ordovician reservoirs in strike-slip fault zones within craton in Shunbei area, Tarim Basin. Oil & Gas Geology, 2023, 44(1): 125–137.

[66] CHEN Honghan, WU You, ZHU Hongtao, et al. Eogenetic karstification and reservoir formation model of the Middle-Lower Ordovician in the northeast slope of Tazhong uplift, Tarim Basin. Acta Petrolei Sinica, 2016, 37(10): 1231–1246.

[67] OUYANG S Q, LYU X X, QUAN H, et al. Evolution process and factors influencing the tight carbonate caprock: Ordovician Yingshan Formation from the northern slope of the Tazhong uplift, Tarim Basin, China. Marine and Petroleum Geology, 2023, 147: 105998.

[68] FAN Tailiang, GAO Zhiqian, WU Jun. Formation and modification of deep-burial carbonate rocks and orderly distribution of multi-type reservoirs in the Tarim Basin. Earth Science Frontiers, 2023, 30(4): 1–18.

[69] LI B, GOLDBERG K. Diagenesis and reservoir quality of Cambrian carbonates in the Tarim Basin, northwestern China. Journal of Asian Earth Sciences, 2022, 223: 104972.

[70] JIU B, HUANG W H, MU N N, et al. Effect of hydrothermal fluids on the ultra-deep Ordovician carbonate rocks in Tarim Basin, China. Journal of Petroleum Science and Engineering, 2020, 194: 107445.

[71] CHEN Lanpiao, LI Guorong, WU Zhangzhi, et al. Study on the Ordovician hydrothermal action at Late Hercynian in the southeast slope of Tahe Oilfield, Tarim Basin. Natural Gas Geoscience, 2017, 28(3): 410–419.

[72] LIU Baozeng. Analysis of main controlling factors of oil and gas differential accumulation in Shunbei area, Tarim Basin-taking Shunbei No.1 and No.5 strike-slip fault zones as examples. China Petroleum Exploration, 2020, 25(3): 83–95.